



A comprehensive SKA Survey of lensing clusters and lensed galaxies

M. Pandey-Pommier ¹, J. Mckean ², I. Harrison ³ and C. Cress ⁴

¹*Pole Scientific, University Catholic of Lyon- University of Lyon, 10 place des Archives 69288, Lyon, France*

²*University of Pretoria, Private Bag x20 Hatfield 0028, South Africa*

³*School of Physics and Astronomy, Cardiff University, CF24 3AA, United Kingdom*

⁴*Mathematical Sciences, University of South Africa, Christiaan de Wet Rd, Florida, 1709, Johannesburg, South Africa*

E-mail: mamtapommier@gmail.com, john.mckean@up.ac.za,
harrisoni@cardiff.ac.uk, cresscm@unisa.ac.za

Galaxy clusters act as powerful gravitational lenses that provide a unique laboratory for studying the distribution of dark matter and the properties of faint background galaxies. In the radio regime, cluster lensing studies remain largely unexplored due to the intrinsically low surface density of background radio sources, which limits the number of detectable lensed systems and constrains the application of cluster-scale lensing to cosmological and astrophysical investigations. In this paper, we outline how the SKA will transform cluster lensing studies through its unprecedented sensitivity, angular resolution, and survey speed. These capabilities will enable dense sampling of lensed background radio sources and high-fidelity reconstruction of cluster mass distributions, while revealing a previously inaccessible population of faint (μJy -level) galaxies, primarily at $z \sim 1 - 5$. We focus on three key science goals: (i) constraining dark matter substructure in galaxy clusters through improved strong-lensing constraints, (ii) characterising the non-thermal baryonic components of the intracluster medium, and (iii) building statistically significant samples of μJy -level lensed galaxies to study star formation and active galactic nuclei activity across cosmic time (primarily at $z \sim 1 - 5$). Together, these advances will establish cluster-scale radio lensing as a powerful probe of structure formation and galaxy evolution in the SKA era.

1 Introduction

Gravitational lensing is an astronomical phenomenon where the gravitational pull of a dense cosmic object, such as a cluster or galaxy, bends the light from a distant background galaxy. This bending of light gives rise to the curvature of spacetime, resulting in multiple images of the distant galaxy (Zwicky, 1937). Depending on the alignment of the distant galaxy and mass distribution of the lensing system, lensing can manifest in various forms, including strong and weak lensing (Meylan et al., 2004). This phenomenon can produce a range of effects, including distorted images, large arc-like or multiple symmetric structures, or Einstein rings, all of which align along the critical curves of the lensing system (Schneider, 2006; Virbhadra et al., 1998).

Galaxy clusters represent the most massive gravitationally bound systems in the Universe and are among the most powerful gravitational lenses known due to their enormous mass (up to $10^{15} M_{\odot}$), a critical requirement for cosmic lensing. While $\sim 70 - 80\%$ of the total mass in massive galaxy clusters is dominated by dark matter, followed by $\sim 15 - 20\%$ of hot gas ($T \sim 10^{15} \text{K}$) in the Intra Cluster Medium (ICM), the remaining is in the form of a few percent of baryonic matter in the galaxies. The dark matter dominates the cluster potential and is expected to be collision less in nature, interacting through gravity only (Bradač et al., 2006; Natarajan et al., 2024). Cold Dark Matter predicts significant sub-structure in halos, and lensing provides one of the few probes of this prediction (Powell et al., 2025). Through strong and weak lensing, clusters provide direct constraints on the projected total mass distribution, enabling detailed studies of dark matter structure and its interaction with baryonic components. Strong gravitational lensing in clusters enables us to probe the high-redshift galaxies, including those from the epoch of reionization $z \sim 6$ and beyond, that would otherwise be too faint to observe. The magnified lensed images offer critical insights into galaxy evolution and star formation in the distant universe (Schneider, 2006; Umetsu et al., 2016; Ueda et al., 2019). In addition, lensing analyses provide key insights into the internal structure of galaxy clusters, including their substructures and mass distributions. Combined with X-ray and radio observations, these analyses offer a more comprehensive view of the baryonic and dark matter components of clusters, as well as their complex interplay (Zitrin et al., 2015; Pandey-Pommier et al., 2016; Natarajan et al., 2024).

This work is motivated by three fundamental questions:

- What is the distribution and level of substructure in the dark matter halos of lensing clusters?
- How do baryonic processes such as hot gas dynamics and non-thermal plasma relate to the underlying dark matter potential?
- What is the nature of faint radio-emitting galaxies at intermediate and high redshift, and how are they magnified by cluster lenses?

To address these questions, cluster lensing observations require both high-resolution mass mapping and a sufficiently dense background population of detectable sources. Extensive multi-wavelength observational campaigns such as the ESO Hamburg survey (Wisotzki et al., 1996), CfA-Arizona-ST-LENS-Survey (CASTLES by (Muñoz et al., 1999); Frontier Fields (FF) program using the HST (Lotz et al., 2017), ALMA (Hezaveh et al., 2013), JWST (Castellano et al., 2023), and MUSE/VLT

(Richard et al., 2015) have significantly deepened our understanding of lensing clusters' structure, mass profiles, substructure, and their role in magnifying faint, high-redshift background galaxies. In addition, the SDSS survey uncovered hundreds of lensed galaxies and quasars (Bolton et al., 2008; Inada et al., 2012) while wide-field surveys such as DES (DES Collaboration, 2016), and Euclid (Laureijs et al., 2011) have discovered several new gravitational lenses and enabled statistical studies of cluster mass distributions. Collectively, these surveys have expanded the catalog of strong lenses at redshifts as high as, $z \sim 1.98$ and allowed detailed reconstructions of lensed galaxies out to, $z \approx 10$ (Negrello et al., 2010; Vieira et al., 2013; Finner et al., 2025).

At radio wavelengths, galaxy-galaxy gravitational lensing has been extensively explored through surveys such as the Jodrell Bank–VLA Astrometric Survey (JVAS) and the Cosmic Lens All Sky Survey (CLASS) (Browne et al., 1998; Browne et al., 2003; Patnaik et al., 1992; Myers et al., 1995; Myers et al., 2003; Jackson et al., 1995; McKean et al., 2015). These surveys used flat-spectrum radio sources to discover the majority of known radio gravitational lenses. To date, approximately 300-500 lensing systems have been identified across different mass scales (galaxies and groups), though only about $\sim 10\%$ involve radio-loud background sources. These surveys have enabled lensing investigations up to redshifts of $z \sim 1.5$ (Jackson et al., 1995; McKean et al., 2007), although they typically rely on ancillary optical or infrared data for redshift determination. In addition, recent studies on lensing cluster-galaxy systems with the SKA pathfinders, GMRT, and LOFAR confirmed the dynamical state of the lensing clusters (Pandey-Pommier et al., 2016) and at higher frequencies ($\sim 1 - 6$ GHz) and resolution (< 1.8 arcsec) with the JVLA discovered several (~ 20) radio-emitting lensed galaxies up to ($z \sim 2$) (van Weeren et al., 2016; Heywood et al., 2021). However, these cluster-scale lensing studies in the radio regime remain vastly under-utilised, especially limited to a couple of FF clusters up to ($z \sim 0.545$). In general, current radio facilities are still limited by sensitivity and angular resolution, resulting in a small number of detected lensed sources and insufficient background source density for detailed cluster mass reconstruction (McKean et al., 2015; Pandey-Pommier et al., 2018; Heywood et al., 2021). These limitations reflect both selection biases and instrumental constraints, as present-day radio surveys are optimised for compact lens configurations and are not yet sensitive enough to routinely detect the μJy -level background source population required for robust cluster-scale lensing analyses. Further, while gravitational lensing robustly constrains the total projected mass distribution, it does not directly probe gas dynamics. Instead, multi-wavelength observations combining lensing (mass), X-ray emission (hot gas), and radio emission (non-thermal plasma) are required to disentangle the baryonic and dark matter components of clusters. Furthermore, at ($> z \sim 0.54$), our understanding of mass distributions and the dark–baryonic matter interplay in lensing clusters still heavily depends on optical, infrared, and mm-observations, as radio observations at these redshifts remain largely unexplored (Natarajan et al., 2024; Finner et al., 2025).

In this paper, we focus on cluster-galaxy lensing as a probe of dark matter substructure and the population of faint lensed radio sources. We investigate how increased source density and improved angular resolution of SKA will enable more accurate mass reconstruction of cluster lenses and open the possibility of building statistically meaningful samples of μJy -level lensed galaxies at $z \sim 1 - 5$, providing new constraints on galaxy evolution in dense environments. Throughout the paper, we adopt a ΛCDM cosmology with $H_0 = 70 \text{ km s}^{-1}\text{Mpc}^{-1}$, $\Omega_M = 0.3$ and $\Omega_\Lambda = 0.7$.

2 Baryonic and Dark matter interplay in Lensing clusters

2.1 Tracing Matter Distribution via Low-Frequency Radio Emission in Lensing Clusters

Low-frequency radio observations are crucial for understanding the distribution of matter, non-thermal component of the ICM, and the dynamical state in lensing galaxy clusters. The degree of merger activity in a cluster's central region determines the type of non-thermal radio emission observed in the ICM, which is typically faint and more effectively detected at low radio frequencies due to its steep spectral nature ($\alpha \lesssim -1.3$). It is important to note here that these radio-emitting structures are not unique to lensing-selected clusters, but instead are a general property of massive and dynamically active galaxy clusters. Lensing clusters are therefore best understood as a biased subset of the most massive and centrally concentrated clusters, which are particularly efficient laboratories for studying both gravitational lensing and diffuse radio emission due to their high total mass and strong gravitational potential.

Depending on their physical origin and location within the broader class of massive cluster, the non-thermal radio emissions are classified into the strongly polarized peripheral 'relics' (a few kpc - Mpc scale) and central fossil plasma 'Phoenix' (a few kpc scale), both of which arise from shocks or compression within the ICM. Additionally, turbulence induced by mergers or gas sloshing generates diffuse, unpolarized centrally located radio structures, such as, haloes (> 500 kpc, up to or beyond 1 Mpc) in dynamically unrelaxed, elongated 'non-cool core' (NC) clusters, and more compact mini-haloes (< 500 kpc) in relaxed, compact 'cool core' (CC) clusters (Feretti et al., 2012). In addition, relaxed CC clusters tend to host a central radio-loud bright cluster galaxy (BCG), while non-relaxed NCC clusters often contain multiple radio-emitting ellipticals in their center associated with the sub-group undergoing merging activity.

Over the past decade, SKA pathfinder surveys such as uGMRT, JVLA, LOFAR and MeerKAT, have significantly expanded the number of known diffuse radio sources in clusters, including rare ultra-steep spectrum radio halos (USSRHs), thanks to their μ Jy-level sensitivity down to 110 MHz. USSRHs are characterised by very steep spectral indices ($\alpha \lesssim -1.5$), making them preferentially detectable at low radio frequencies. They are thought to trace less energetic cluster mergers and therefore provide important probes of particle acceleration mechanisms and the dynamical evolution of galaxy clusters (Venturi et al., 2008; Cassano et al., 2010; Bonafede et al., 2012; Kale et al., 2013, 2015; Pandey-Pommier et al., 2013; Brunetti and Jones, 2014; Pandey-Pommier et al., 2016; van Weeren et al., 2019; Cuciti et al., 2021; Knowles et al., 2022; Phuravhathu et al., 2025). They therefore provide key constraints on particle acceleration efficiency and the dynamical state of clusters that may otherwise appear relaxed at higher frequencies. However, the observed abundance of these systems remains lower than theoretical expectations, highlighting a discrepancy between predicted and observed populations of diffuse radio emission (Cassano et al., 2015). The first-ever targeted low-frequency radio survey of lensing clusters (up to $z \sim 0.545$) was conducted by (Pandey-Pommier et al., 2016), finding relics, halos, and mini-halos in those systems, similar to those in non-lensing clusters. However, compared to non-lensing clusters, lensing clusters tend to be massive (often $\geq 0.5 \times 10^{15} M_{\odot}$) and generally show high central mass concentrations and relaxed CC nature (with few exceptions from merging clusters, e.g., MACS J0717.5 + 3745) (ref. Fig.1). The discrepancies in radio halo number counts is largely driven by current limitations in

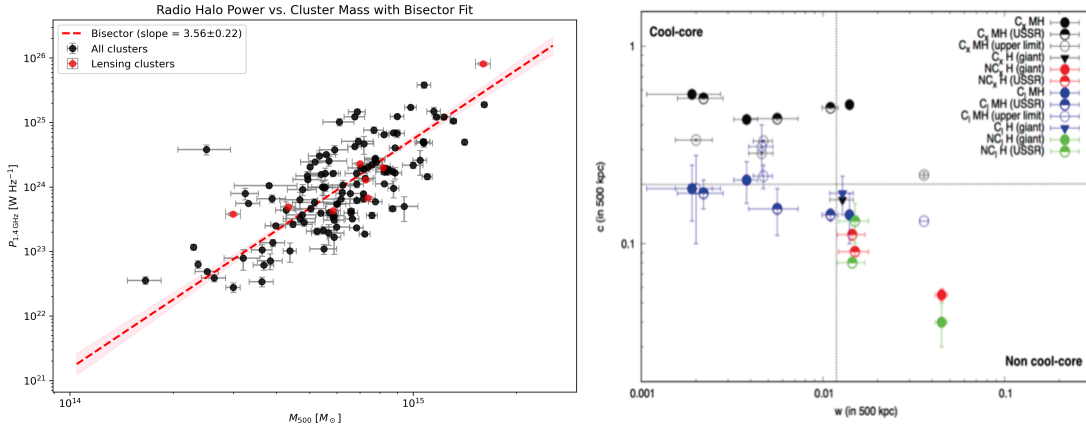


Figure 1: *Left panel:* Radio power-mass distribution diagram for the clusters with known radio halos from literature for lensing (red) and non-lensing (black) clusters. *Right panel:* Dark-baryonic matter coupling in lensing galaxy clusters. The non-detection limits are marked as ‘UL’, radio halo as ‘RH’, X-ray concentration in cool-core as ‘Cx’, X-ray concentration in non cool-core as ‘NCx’, concentration in total mass map via lensing analysis as ‘CI’ in cool-cores and ‘NCI’ in non cool-core clusters (Pandey-Pommier et al., 2016).

sensitivity and surface brightness detection, which the SKA will address by enabling a statistically complete census of diffuse radio emission in galaxy clusters.

2.2 Gas–Mass Alignment and the Dark–Baryonic Interplay in Lensing Galaxy Clusters

Gravitational lensing provides a direct and robust reconstruction of the projected total mass distribution in galaxy clusters, making it one of the most powerful probes of the underlying dark matter potential and of the spatial relationship between dark and baryonic matter. It is important to note that lensing clusters are not representative of the general cluster population; rather, they constitute a biased subset toward high masses and centrally concentrated mass distributions, which enhance their lensing cross-sections, increase their detectability in lensing surveys, and amplify observable signatures of baryonic–dark matter interplay.

Multiwavelength observations combining gravitational lensing (total mass), X-ray emission (hot ICM), and radio emission (non-thermal plasma) are essential to fully characterise the dynamical state of these systems. While lensing and X-ray data provide constraints on the collisional (gas) and collisionless (dark matter) components, radio observations offer an additional and independent tracer of non-thermal processes driven by cluster dynamics. In particular, diffuse radio emission such as halos, mini-halos, and relics traces turbulence, merger-driven shocks, and particle acceleration within the ICM, while spectral index variations provide information on the energy distribution and ageing of relativistic electrons. In addition, radio emission associated with AGN in BCGs probes feedback processes that regulate the thermodynamic state of the cluster core. These radio observables therefore provide complementary and physically independent constraints on cluster dynamical activity that are not accessible through lensing or X-ray data alone. Morphological diagnostics derived from X-ray and lensing maps, such as the concentration parameter (c) and centroid shift (w), are widely used to quantify cluster relaxation states (Cassano et al., 2010; Kale et al., 2015; Pandey-Pommier et al., 2016). As illustrated in Fig. 1 (left panel) lensing clusters occupy

the high-mass end of the radio power–mass relation. This reflects the selection bias toward massive and centrally concentrated systems with enhanced lensing cross-sections. In Fig. 1 (right panel), relaxed CC systems exhibit centrally concentrated X-ray emission and well-aligned mass and gas peaks, indicating a close spatial correspondence between baryonic and dark matter distributions. In contrast, non-relaxed NCC systems show disturbed morphologies, with significant offsets between the X-ray peak and the lensing-derived mass centroid. These offsets arise from merger-induced shocks and bulk gas motions, which affect the collisional baryonic component, leaving the collisionless dark matter distribution largely unaffected. The morphology, and spectral properties of these radio components provide a complementary diagnostic of cluster assembly and dynamical activity, complementary to X-ray and lensing-based measures.

Owing to their large masses and strong gravitational potentials, lensing clusters provide a unique opportunity to study the coupling between dark matter, baryons, and non-thermal plasma, enabling direct comparison with baryonic tracers across wavelengths. Current progress, however, is constrained by limited sensitivity and angular resolution for detecting faint diffuse radio emission and mapping its connection to cluster mass substructures.

2.3 Probing Cold Gas Reservoirs in Lensing Galaxy Clusters

Relaxed CC clusters are characterised by a central concentration of cold molecular gas, which provides a striking contrast to the hotter X-ray emitting ICM in the outer regions (Fabian, 1994; Edge, 2001). These regions are strongly influenced by feedback from the central AGN, which regulates the thermodynamic state of the ICM through a balance between radiative cooling and mechanical heating from jets and outflows. In low-entropy systems, reduced cooling times allow gas to condense out of the hot phase, forming molecular reservoirs that can fuel both star formation and AGN activity. This cooling–feedback cycle is therefore directly linked to the baryonic evolution of the central BCGs and may correlate with lensing efficiencies through their association with dynamically relaxed, centrally concentrated systems. Recent observations by (Castignani et al., 2020) investigated molecular gas in 18 BCGs belonging to the CLASH lensing cluster sample over the redshift range $z \approx 0.2 - 0.9$, using CO line observations (Fig. 2). Only one system (RXJ1532.9+3021) shows a robust detection of a substantial molecular gas reservoir, while four additional BCGs exhibit tentative detections. The remaining 13 systems show very low molecular gas-to-stellar mass ratios ($M_{\text{H}_2}/M_{\star} < 0.1$), indicating that most BCGs in this sample are relatively poor in cold molecular gas. The detected molecular gas masses span $M_{\text{H}_2} \sim 10^{10} - 10^{11} M_{\odot}$, with RXJ1532.9+3021 exhibiting a particularly large reservoir of $M_{\text{H}_2} = (8.7 \pm 1.1) \times 10^{10} M_{\odot}$ and an associated star formation rate (SFR) exceeding $100 M_{\odot} \text{ yr}^{-1}$. The left panel of Fig. 2 shows a weak but important redshift dependence with higher-redshift systems tend to have less constrained molecular gas measurements due to observational sensitivity limits, rather than intrinsic absence of gas. This highlights the need for larger and more sensitive samples, particularly at higher redshift, to determine whether the observed trends reflect true evolution or selection effects. These findings are consistent with the picture that most gas-rich BCGs are preferentially located in cool-core systems, as suggested by previous studies (Edge, 2001). BCGs with high SFRs tend to host significant H_2 masses and display clumpy, filamentary morphologies, underscoring the role of central entropy and cooling flows in driving molecular gas accumulation. At the same time, mechanical feedback

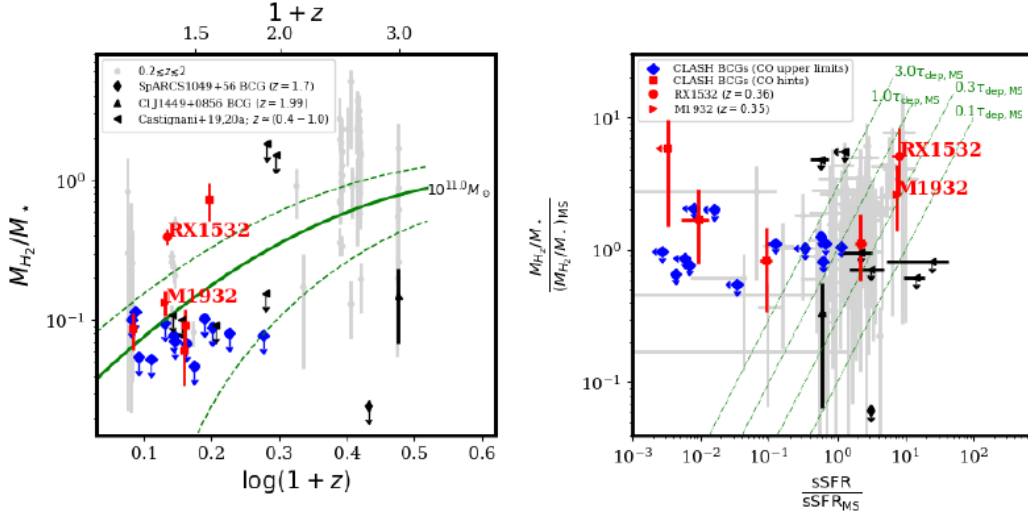


Figure 2: Molecular gas properties of distant BCGs in lensing clusters observed in CO (*Left panel*) with IRAM and their star formation rate (*Right panel*), from (Castignani et al., 2020)

from the central AGN, through radio jets and gas sloshing, plays a key role in regulating gas inflow and suppressing cooling. BCGs with low central entropy frequently exhibit both emission-line signatures of ongoing star formation (Fogarty et al., 2015) and evidence of AGN activity (Hogan et al., 2015), suggesting a common fuelling source linked to the hot ICM and a close interplay between cooling flows and AGN feedback. In relaxed cool-core systems, this AGN feedback cycle can explain the coexistence of molecular gas, star formation, and AGN activity in a subset of low-entropy clusters, while efficient feedback heating keeps many other systems relatively gas poor.

Radio observations provide an independent probe of this feedback cycle. In the CLASH sample, (Heng et al., 2018) find that 1.5 GHz radio power in BCGs spans $P_{1.5\text{GHz}} \sim 2 \times 10^{23}$ to 10^{26} W Hz^{-1} , with a statistically significant positive correlation with SFR and a negative correlation with ICM entropy. These results indicate that stronger AGN activity is preferentially associated with systems where cooling is more effective, consistent with a self-regulated feedback scenario. From a lensing perspective, these baryonic processes are particularly relevant because low-entropy, dynamically active cores often correspond to high central mass concentrations and enhanced lensing efficiency. However, current observational constraints remain incomplete as: (i) the sample size of molecular gas measurements in lensing-selected BCGs is small, (ii) the redshift coverage is limited, particularly beyond $z \gtrsim 0.5$, and (iii) sensitivity limitations prevent detection of low-mass gas reservoirs in typical systems. In addition, most current surveys lack uniform frequency coverage for simultaneously tracing both molecular gas and atomic gas in the same cluster environments. The SKA will overcome these limitations by enabling significantly deeper observations.

2.4 Background Lensed Galaxies

Background-lensed galaxies in the environments of massive lensing clusters detected as unresolved radio sources or arcs, offer valuable insights into galaxy formation and evolution at high redshifts,

(Pandey-Pommier et al., 2018). Using deep JVLA observations of the massive FF lensing cluster MACS J0717.5+3745, (van Weeren et al., 2016) reported the detection of several strongly lensed background radio sources out to $z \sim 2.1$. In a complementary study, (Heywood et al., 2021) conducted high-resolution radio imaging on MACS J0717.5+3745 and MACS J1149.5+2223, at 3 GHz and 6 GHz using the JVLA. These observations achieved sub-arcsecond resolution and μJy -level sensitivity, reaching RMS noise levels of $5\text{--}10 \mu\text{Jy beam}^{-1}$, enabling detection of both cluster-associated and gravitationally lensed background galaxies out to $z \sim 1.2$. The detected lensed sources exhibit flux densities typically ranging from a few μJy to 100s of μJy , with many detections near the $10\text{--}30 \mu\text{Jy}$ level, barely at the detection limit of JVLA. After correcting for lensing magnification, these correspond to intrinsically low-luminosity radio sources in the μJy -level regime. However, a discrepancy in the redshift distribution of detected lensed sources was observed between studies, primarily due to (Heywood et al., 2021) adopting median magnification values, whereas (van Weeren et al., 2016) used mean values. Based on radio morphology, spectral properties, and multiwavelength counterparts, the lensed radio galaxies observed in the FF fall into star-forming galaxies, typically late-type or irregular systems, exhibiting compact, unresolved radio emission consistent with non-thermal synchrotron radiation. Their optical and near-infrared counterparts often show blue continuum and clumpy, irregular morphologies, particularly at redshifts $z > 1$. In addition, a subset of sources is associated with red, compact galaxies, likely quiescent ellipticals hosting low-luminosity AGN that show weak radio emission and little to no star formation activity, possibly indicating radio-mode AGN feedback. A few galaxies also showed an intermediate nature where both AGN and star formation features were observed simultaneously. Such sources may represent transition phases in galaxy evolution, possibly linked to episodes of AGN triggering, feedback-regulated star formation, or merger-driven gas inflows in dense environments. However, current observations remain limited to determine whether these hybrid sources correspond to a distinct evolutionary stage or arise from multiple physical mechanisms.

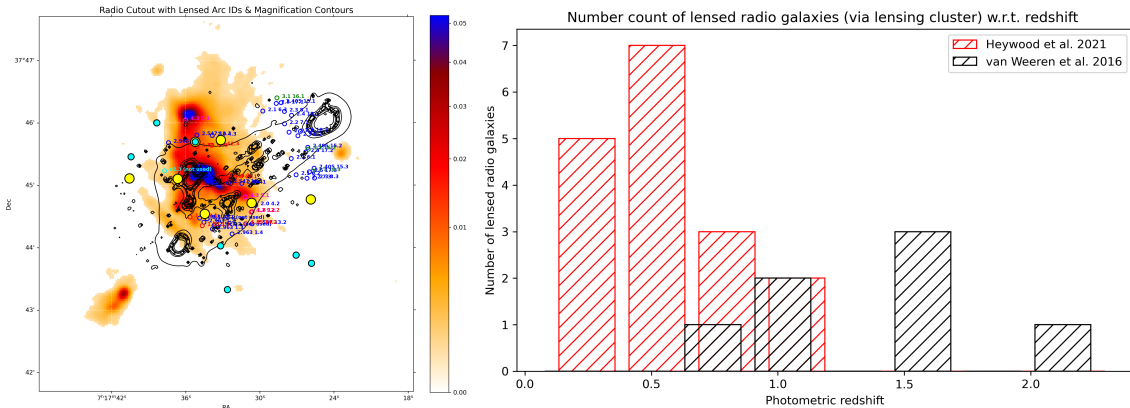


Figure 3: *Left panel:* Gravitational Lensing in MACSJ0717.5+3745 cluster with total mass map in black contours overlaid on GMRT data (Pandey-Pommier et al., 2016) showing JVLA radio lensed galaxies in cyan (van Weeren et al. (2016)) and yellow (Heywood et al., 2021)) circles. *Right panel:* Radio lensed galaxies discovered in massive clusters environments.

3 SKA capabilities and multi-wavelength synergies

As discussed in previous sections, despite several advances, current radio lensing studies still face two major observational challenges: (1) insufficient sensitivity to detect large numbers of faint background sources, and (2) limited angular resolution for resolving multiple lensed images in cluster environments. As a result, constraints on cluster substructure and high-redshift lensed galaxy populations remain incomplete in the radio band. With μJy -level sensitivity, sub-arcsecond resolution, and wide-field survey capability, the SKA will increase the number density of detectable background radio sources by orders of magnitude, enabling high-fidelity reconstruction of cluster mass distributions and the identification of statistically significant samples of strongly lensed galaxies (Prandoni and Seymour, 2014; McKean et al., 2015; Pandey-Pommier et al., 2016, 2018). These advances will establish cluster-scale radio lensing as a powerful probe of dark matter substructure, baryonic processes, and galaxy evolution through gravitational magnification.

As shown in Fig. 4, SKA AA* and AA4 arrays and current path-finders are already capable of detecting diffuse synchrotron emission from cluster haloes and relics in massive systems, while higher-frequency instruments such as the JVLA provide the angular resolution required to identify compact lensed radio galaxies. However, existing observations remain sensitivity limited, particularly for faint μJy -level background galaxies and high-redshift diffuse radio emission. SKA-LOW and SKA-MID will overcome these limitations by combining high surface-brightness sensitivity with sub-arcsecond resolution, enabling simultaneous studies of cluster radio haloes, relics, and

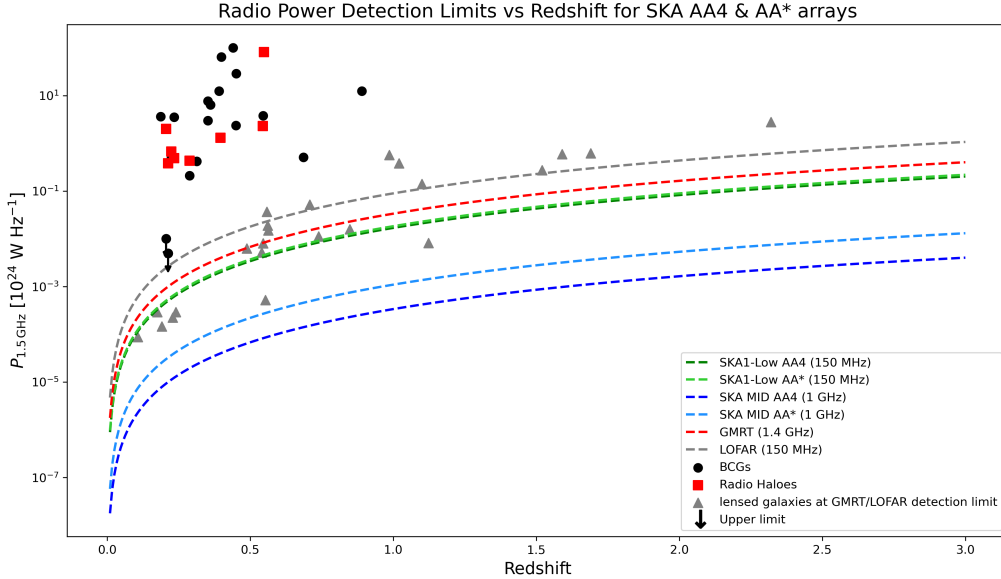


Figure 4: Radio array sensitivities in comparison to the SKA AA4 and AA* arrays, showing the radio power at 1 GHz detectable with a sensitivity of $1 \mu\text{Jy}$ (defined as $3 \times$ the RMS noise), as computed using the SKA sensitivity calculator: sensitivity-calculator.skao.int. The black, red, and grey points indicate radio luminosities currently measured in BCGs, radio haloes observed with GMRT and LOFAR, and lensed distant galaxies with the JVLA, respectively, in lensing clusters (Heng et al., 2018; Pandey-Pommier et al., 2016; van Weeren et al., 2016; Heywood et al., 2021).

strongly lensed galaxies across a broad redshift range. This will allow direct investigation of the interplay between cluster dynamics, dark matter structure, AGN feedback, and galaxy evolution across cosmic time (McKean et al., 2015; Pandey-Pommier et al., 2018). A major advance enabled by SKA (AA* and AA4) arrays will be the detection of large populations of faint lensed radio galaxies at $z \sim 1 - 5$, many of which are currently inaccessible. These observations will constrain the faint end of the radio luminosity function and provide new insights into the co-evolution of star formation and AGN activity in low-luminosity galaxies. In addition, high-resolution radio imaging of multiply imaged systems will improve constraints on cluster substructure and the distribution of dark matter within cluster cores.

Beyond continuum observations, SKA spectral-line observations will probe the cold gas content and kinematics of cluster galaxies through H I 21-cm transition and low- J CO emission, enabling measurements of gas reservoirs, inflows/outflows, and star-formation fueling in cluster galaxies. These data will be key to understanding cooling flows, AGN feedback, and star-formation regulation in cluster cores (Pandey-Pommier et al., 2026b). At higher frequencies, SKA Band 5 may also detect dense gas tracers such as HCN and HCO⁺ in highly magnified, strongly lensed systems at $z \gtrsim 5$, offering rare constraints on dense star-forming gas in the early Universe (Pandey-Pommier et al., 2026a). Combined with lensing magnification, this will enable detailed studies of the interstellar medium in faint, high-redshift galaxies near the peak of cosmic star formation and potentially into the epoch of reionization.

The scientific return of SKA observations will be significantly enhanced through multi-wavelength synergies with forthcoming facilities. Optical/near-IR surveys from Euclid, LSST, JWST and WST (Mainieri et al., 2024) will provide photometric and spectroscopic redshifts, stellar masses, and detailed morphological information for lensed galaxies and cluster members (Laureijs et al., 2011; Castellano et al., 2023). ATHENA (X-rays) will trace the thermodynamic state of the hot ICM, while ALMA/NOEMA will probe the molecular gas component through CO imaging and spectroscopy (Barcons et al., 2017; Wootten and Thompson, 2009). Together, these datasets will deliver a comprehensive multi-phase view of baryons in clusters, linking total mass distributions from lensing to hot, cold, and non-thermal components. Further, in combination with optical weak-lensing surveys, SKA data will further improve cluster mass reconstructions and tighten constraints on structure formation and the evolution of massive halos across cosmic time.

4 Summary and conclusion

In this chapter, we have shown that galaxy clusters are powerful gravitational lenses and key laboratories for studying the interplay between dark matter, baryons, and non-thermal processes through radio observations. While current data already reveal diffuse emission, gas–mass offsets, and a limited population of lensed radio galaxies, progress is constrained by sensitivity and resolution limits. The SKA will overcome these challenges with μ Jy sensitivity and high angular resolution, enabling detailed studies of cluster substructure, diffuse ICM emission, and large samples of strongly lensed galaxies beyond $z \sim 2$. Additionally, the spectral-line capabilities of SKA will provide direct constraints on the cold gas content and kinematics of cluster galaxies. The SKA Band 5 may also enable detections of dense molecular gas tracers (HCN and HCO⁺) in highly magnified systems and

star-forming distant lensed galaxies at $z \gtrsim 5$. Together with future multi-wavelength facilities, the SKA will provide a comprehensive view of cluster evolution and lensed galaxy populations across cosmic time.

Author Ordering

Authors for this chapter are ordered according to their overall level of expertise and contribution, in line with that expected for a small author list publication.

Acknowledgements

We thank the anonymous referee for their constructive comments and insightful suggestions, which helped improve the clarity of this manuscript.

References

- X. Barcons et al. *Astronomische Nachrichten*, 338:153–158, 2017. doi: 10.1002/asna.201713323.
- A. Bolton, S. Burles, Koopmans, et al. *The Astrophysical Journal*, 682:964, 2008. doi: 10.48550/arXiv.0805.1931.
- A. Bonafede, M. Brüggen, R. van Weeren, and et al. *Monthly Notices of the Royal Astronomical Society*, 426:40, Oct 2012. doi: 10.1111/j.1365-2966.2012.21570.x.
- M. Bradač, D. Clowe, A. H. Gonzalez, and et al. *The Astrophysical Journal*, 652(2):937–947, Dec 2006. doi: 10.1086/508601.
- I. Browne, P. Wilkinson, N. Jackson, and et al. *Monthly Notices of the Royal Astronomical Society*, 341:13–32, 2003. doi: 10.1046/j.1365-8711.2003.06257.x.
- I. W. A. Browne, N. J. Jackson, P. Augusto, and et al. *Astrophysics and Space Science Library*, 226: 323–332, 1998. doi: 10.1007/978-94-011-5238-9_57.
- B. Brunetti and T. Jones. *International Journal of Modern Physics D*, 23:1430007-98, 2014. doi: 10.1142/S0218271814300079.
- R. Cassano, S. Ettori, S. Giacintucci, and et al. *The Astrophysical Journal Letters*, 721:L82, Oct 2010. doi: 10.1088/2041-8205/721/2/L82.
- R. Cassano, G. Bernardi, G. Brunetti, and et al. *Proceedings of Science*, 215, 2015. doi: doi.org/10.22323/1.215.0073.
- M. Castellano, A. Fontana, T. Treu, and et al. *The Astrophysical Journal Letters*, 948:L14, May 2023. doi: 10.3847/2041-8213/accea5.
- G. Castignani, M. Pandey-Pommier, S. L. Hamer, and et al. *A&A*, 640:A65, 2020. doi: 10.1051/0004-6361/202038081.
- V. Cuciti, R. Cassano, G. Brunetti, and et al. *A&A*, 647:16, Aug 2021. doi: 10.1051/0004-6361/202039208.

- DES Collaboration. *Monthly Notices of the Royal Astronomical Society*, 460(2):1270–1299, 2016. doi: 10.1093/mnras/stw641. URL <https://doi.org/10.1093/mnras/stw641>.
- A. C. Edge. *Monthly Notices of the Royal Astronomical Society*, 328:762–782, 2001. doi: 10.1046/j.1365-8711.2001.04802.x.
- A. C. Fabian. *Annual Review of Astronomy and Astrophysics*, 32:277–318, 1994. doi: 10.1146/annurev.aa.32.090194.001425.
- L. Feretti, G. Giovannini, F. Govoni, and et al. *A&A*, 20, May 2012. doi: 10.1007/s00159-012-0054-z.
- K. Finner et al. JWST Discovery of Strong Lensing from a Galaxy Cluster at Cosmic Noon: Giant Arcs and a Highly Concentrated Core of XLSSC 122, Aug 2025.
- K. Fogarty, M. Postman, T. Connor, and et al. *Astrophysical Journal*, 813:117, Nov 2015. doi: 10.1088/0004-637X/813/2/117.
- Y. Heng, T. Paolo, R. van Weeren, and et al. *Astrophysical Journal*, 853:19, feb 2018. doi: 10.3847/1538-4357/aaa421.
- I. Heywood, E. J. Murphy, Jiménez-Andrade, et al. *The Astrophysical Journal*, 910:105, Apr. 2021. doi: 10.3847/1538-4357/abdf61.
- Y. Hezaveh, D. Marrone, C. Fassnacht, and et. al. *Astrophysical Journal*, 767:11, Apr. 2013. doi: 10.48550/arXiv.1303.2722.
- M. Hogan, A. Edge, J. Hlavacek-Larrondo, and et al. *Monthly Notices of the Royal Astronomical Society*, 453:1223, October 2015. doi: 10.1093/mnras/stv1518.
- N. Inada, M. Oguri, M. Shin, and et al. *The Astronomical Journal*, 143:119, 2012. doi: 10.1088/0004-6256/143/5/119.
- N. Jackson, A. G. de Bruyn, S. Myers, and et al. *Monthly Notices of the Royal Astronomical Society*, 274:L25, 1995. doi: 10.1093/mnras/274.1.L25.
- R. Kale, T. Venturi, S. Giacintucci, and et al. *Astronomy & Astrophysics*, 557:18, Sep 2013. doi: 10.1051/0004-6361/201321515.
- R. Kale et al. *Astronomy & Astrophysics*, 579:22, Jul 2015. doi: 10.1051/0004-6361/201525695.
- K. Knowles et al. *Astronomy & Astrophysics*, 657:A56, 2022. doi: 10.48550/arXiv.2111.05673.
- R. Laureijs et al. *arXiv e-prints*, 2011. URL <https://arxiv.org/abs/1110.3193>.
- J. M. Lotz, A. Koekemoer, D. Coe, and et al. *Astrophysical Journal*, 837:97, Mar. 2017. doi: 10.3847/1538-4357/837/1/97.
- V. Mainieri et al. *arXiv e-prints*, art. arXiv:2403.05398, Mar. 2024. doi: 10.48550/arXiv.2403.05398.

- J. McKean, I. Browne, N. Jackson, and et al. *Monthly Notices of the Royal Astronomical Society*, 377:430–440, 2007. doi: 10.48550/arXiv.astro-ph/0702362.
- J. McKean et al. *Monthly Notices of the Royal Astronomical Society*, 451(4):4386–4397, 2015. doi: 10.1093/mnras/stv1157.
- G. Meylan, P. Jetzer, N. North, and et al. *Gravitational lensing: strong, weak and micro. Saas-Fee Advanced Course 33*, page 183, 2004. doi: 10.48550/arXiv.astro-ph/0407232.
- J. A. Muñoz, E. E. Falco, C. S. Kochanek, and et al. *Astrophysics and Space Science*, 263(1-4): 51–54, June 1999. doi: 10.1023/A:1002120921330.
- S. Myers, N. Jackson, I. Browne, and et al. *Monthly Notices of the Royal Astronomical Society*, 341:1–12, 2003. doi: 10.1046/j.1365-8711.2003.06256.x.
- S. T. Myers, C. D. Fassnacht, S. G. Djorgovski, and et al. *The Astrophysical Journal*, 447(1):L5, Jul 1995. doi: 10.1086/309556.
- P. Natarajan, L. Williams, M. Bradač, and et al. *Space Science Reviews*, 220:19, Feb. 2024. doi: 10.1007/s11214-024-01051-8.
- M. Negrello, R. Hopwood, G. De Zotti, and et al. *Science*, 330:800, 2010. doi: 10.1126/science.1193420.
- M. Pandey-Pommier, J. Richard, F. Combes, and et al. *A&A*, 557:A117, Jun 2013. doi: 10.1051/0004-6361/201321809.
- M. Pandey-Pommier et al. Tracing gas outflows in molecular hydrogen emission-rich galaxies with the ska. In *Advancing Astrophysics with the SKA – II (AASKAII)*. 2026a. arXiv search: Report number AASKAII/Pandey-Pommier01.
- M. Pandey-Pommier et al. Uncovering neutral hydrogen clouds in radio galaxies in the ska era. In *Advancing Astrophysics with the SKA – II (AASKAII)*. 2026b. arXiv search: Report number AASKAII/Pandey-Pommier03.
- M. Pandey-Pommier et al. *SF2A: Proceedings of the Annual meeting of the French Society of Astronomy and Astrophysics*, 2016. doi: 10.48550/arXiv.1612.00225.
- M. Pandey-Pommier, J. Richard, and et al. *French SKA White Book, Chapter 2.1.8*, 2018. doi: 10.48550/arXiv.1712.06950.
- A. R. Patnaik, I. W. A. Browne, and et al. *Monthly Notices of the Royal Astronomical Society*, 259 (1):1P–4P, nov 1992. doi: 10.1093/mnras/259.1.1P.
- D. Phuravhathu et al. *MNRAS*, 542:1544–1561, 2025. doi: 10.1093/mnras/staf1315.
- D. M. Powell et al. *Nature Astronomy*, Oct. 2025. doi: 10.48550/arXiv.2510.07382.
- I. Prandoni and N. Seymour. *Proceedings 'Advancing Astrophysics with the SKA' PoS(AASKA14)067*, Apr 2014. doi: 10.48550/arXiv.1412.6512.

- J. Richard, V. Patricio, J. Martinez, and et al. *Monthly Notices of the Royal Astronomical Society*, 446:L16–20, Jan. 2015. doi: 10.1093/mnras/lu150.
- P. Schneider. *Springer Lecture Notes in Physics*, 2006.
- S. Ueda et al. *Astrophysical Journal*, 870(2):L19, 2019. doi: 10.3847/2041-8213/ab13b5.
- K. Umetsu et al. *Monthly Notices of the Royal Astronomical Society*, 463(2):2107–2124, 2016. doi: 10.1093/mnras/stw2075.
- R. van Weeren, G. A. Ogrean, C. Jones, and et al. *The Astrophysical Journal*, 817:98, Jan. 2016. doi: 10.3847/0004-637X/817/2/98.
- R. van Weeren, F. de Gasperin, H. Akamatsu, and et al. *Space Sci Rev*, 215:16, Mar 2019. doi: 10.1007/s11214-019-0584-z.
- T. Venturi, S. Giacintucci, D. Dallacasa, and et al. *Astronomy and Astrophysics*, 484:327, Jun 2008. doi: 10.1051/0004-6361:200809622.
- J. Vieira, D. Marrone, C. Chapman, and et al. *Nature*, 495:344, 2013. doi: 10.1038/nature12001.
- K. S. Virbhadra, D. Narasimha, and S. M. Chitre. *Astronomy and Astrophysics*, 337:1–8, September 1998. doi: 10.48550/arXiv.astro-ph/9801174.
- L. Wisotzki, T. Köhler, D. Groote, and et al. *Astronomy and Astrophysics Supplement series*, 115: 227, 1996.
- A. Wootten and A. R. Thompson. *Proceedings of the IEEE*, 97(8):1463–1471, 2009. doi: 10.1109/JPROC.2009.2020572.
- A. Zitrin et al. *Astrophysical Journal*, 803(1):10, 2015. doi: 10.1088/0004-637X/803/1/10.
- F. Zwicky. *Physical Review*, 51:4, 1937. doi: 10.1103/PhysRev.51.290.